



## Abatement of organics and *Escherichia coli* by N, S co-doped TiO<sub>2</sub> under UV and visible light. Implications of the formation of singlet oxygen (<sup>1</sup>O<sub>2</sub>) under visible light

J.A. Rengifo-Herrera <sup>a</sup>, K. Pierzchała <sup>b</sup>, A. Sienkiewicz <sup>b</sup>, L. Forró <sup>b</sup>, J. Kiwi <sup>a</sup>, C. Pulgarin <sup>a,\*</sup>

<sup>a</sup> SB, ISIC, GGEC, Station 6, Ecole Polytechnique Fédéral de Lausanne, 1015 Lausanne, Switzerland

<sup>b</sup> SB, IPMC, LNNME, Station 3, Ecole Polytechnique Fédéral de Lausanne, 1015 Lausanne, Switzerland

### ARTICLE INFO

#### Article history:

Received 12 September 2008

Received in revised form 20 October 2008

Accepted 25 October 2008

Available online 12 November 2008

#### Keywords:

Heterogeneous photocatalysis

Visible light response

Nitrogen doped TiO<sub>2</sub>

Sulfur doped TiO<sub>2</sub>

### ABSTRACT

Nitrogen and sulfur co-doping has been achieved in the commercial TiO<sub>2</sub> nanoparticles of anatase TKP 102 (Tayca) by grinding it with thiourea and calcinating at 400 °C. The successful substitutional N-doping and cationic/anionic S-doping were validated by XPS measurements. Diffuse reflectance spectroscopy (DRS) showed a marked broadening of the absorption spectrum of the doped material towards the visible range.

Phenol and dichloroacetate (DCA) oxidation and *Escherichia coli* inactivation were achieved under UV illumination using the N, S co-doped TiO<sub>2</sub> powders. Electron spin resonance (ESR) spin-trapping experiments showed that under UV light irradiation, the •OH radicals were the main species responsible for photo-degradation of phenol and *E. coli* abatement. Photo-degradation of DCA was found to be due a direct interaction of the TiO<sub>2</sub> valence band holes (h<sub>VB</sub><sup>+</sup>) with the DCA molecules.

Moreover, under visible light (400–500 nm) illumination of N, S co-doped TiO<sub>2</sub> a complete inactivation of *E. coli* bacteria was observed. In contrast, under such conditions, phenol was only partially degraded, whereas DCA was not at all affected. ESR experiments performed with N, S co-doped TiO<sub>2</sub> powders illuminated with visible light and in the presence of singlet oxygen (<sup>1</sup>O<sub>2</sub>) quencher, TMP-OH, showed the formation of <sup>1</sup>O<sub>2</sub>. This suggests that superoxide radical (•O<sub>2</sub><sup>−</sup>) and its oxidation product, <sup>1</sup>O<sub>2</sub>, were responsible for *E. coli* inactivation by N, S co-doped TiO<sub>2</sub> nanoparticles under visible light.

© 2008 Elsevier B.V. All rights reserved.

## 1. Introduction

Titanium dioxide (TiO<sub>2</sub>) has been widely used as a white pigment and is also considered as the most promising photocatalyst in environmental cleanup, mainly stimulated by the discovery of its water splitting activity under illumination with ultraviolet (UV) light in the early 1970s [1]. However, the overall efficiency of TiO<sub>2</sub> under natural sunlight is limited to the UV-driven activity ( $\lambda < 400$  nm), accounting only to ~4% of the incoming solar energy on the Earth's surface. Therefore, in recent years, shifting of the absorption spectrum of TiO<sub>2</sub> from the UV into the visible light range has attracted a lot of attention [2–4]. In particular, much progress has been achieved in the field of visible-light-active TiO<sub>2</sub> by incorporation of various dopants into its lattice [5,6].

Recently, several authors have demonstrated the photocatalytic activity of N- and S-doped TiO<sub>2</sub> (N, S TiO<sub>2</sub>) in the visible part of the solar spectrum. These materials have been obtained by hydrolytic process using TiCl<sub>4</sub> or titanium tetra-isopropoxide and nitrogen, sulfur and carbon precursors (i.e. ammonia solution, thiourea, ethanol and urea) [7–11]. N-doped commercial TiO<sub>2</sub> powders have also been prepared [12,13]. N, S TiO<sub>2</sub> has been used to degrade air pollutants such as formaldehyde, acetone and NO [14,15]. Most recently, we prepared N, S TiO<sub>2</sub> by a mechanical grinding of TiO<sub>2</sub> with thiourea, which was followed by annealing at 400 °C. This material revealed photocatalytic activity and phototoxicity towards *Escherichia coli* bacteria under illumination with visible light [16].

Several authors have also speculated on the origin of the visible light absorption in N, S TiO<sub>2</sub>. By calculating the band structure of N-doped TiO<sub>2</sub>, Asahi et al. [17] reported that N-doped TiO<sub>2</sub> showed dramatic improvement over undoped TiO<sub>2</sub> in its optical absorption and photocatalytic activity under visible light. Based on their analysis of the density of states, they concluded that the

\* Corresponding author. Tel.: +41 21 693 47 20; fax: +41 21 693 61 61.  
E-mail address: cesar.pulgarin@epfl.ch (C. Pulgarin).

substitution doping of N for O in the anatase  $\text{TiO}_2$  crystal would yield a band-gap narrowing driven by mixing of N 2p states with O 2p states.

In contrast, density functional theory (DFT) calculations and analysis of ESR spectra have suggested that N- and S-doping favors the formation of isolated impurity states localized in the band gap of  $\text{TiO}_2$  rather than the band-gap narrowing, which also accounts for enhanced absorption in the visible part of solar spectrum [18]. This statement has recently been supported by Li et al. [19], who found that at low nitrogen doping levels the absorption in the visible range resulted from the appearance of isolated N 2p states above the  $\text{TiO}_2$  valence band maximum.

Different experimental results have been reported concerning the photocatalytic activity of N- and S-doped titania powders in aqueous media. Two kinds of targets have been used: colored compounds, such as methylene blue and colorless substances, like phenol and 4-chlorophenol. Some authors, while using methylene blue [10,12,17] and phenol or 4-chlorophenol [20–26], found the visible light-driven photocatalytic activity of N, S  $\text{TiO}_2$ . However, Mrowetz et al. [27] pointed out that employment of organic dyes as targets for N-doped  $\text{TiO}_2$  was not suitable because distinguishing between dye-induced photo-sensibilization of  $\text{TiO}_2$  and dye reduction by  $e_{\text{CB}}^-$  occurring at the  $\text{TiO}_2$  nanoparticles surface could be misleading. The promotion of an electron to the conduction band under visible light illumination, thus inducing redox reactions on the N-doped  $\text{TiO}_2$  surfaces, has been suggested. Livraghi et al. [28] proposed that the  $e_{\text{CB}}^-$  could be the species, which participate in the surface redox reactions. Tachikawa et al. [29] reported, while using time-resolved diffuse reflectance spectroscopy, that photogenerated holes in C- and S-doped  $\text{TiO}_2$  under UV-light irradiation could be trapped on the surface and then react with the adsorbed organic compound. On the other hand, Fu et al. demonstrated by ESR spin trapping with nitroxyl spin-trap DMPO that  $\cdot\text{OH}$  radicals can be generated in N-doped  $\text{TiO}_2$  through a nucleophilic attack of  $\text{H}_2\text{O}$  molecules on surface-trapped holes (at oxygen sites of the  $\text{TiO}_2$  surface lattice) [26].

Few studies which dealt with inactivation of bacteria in the presence of N- and S-doped  $\text{TiO}_2$  under visible light irradiation suggested that reactive oxygen species (ROS) were responsible for the bacterial inactivation [30–32]. Recently, Mitoraj et al. reported that C-doped  $\text{TiO}_2$  and  $\text{TiO}_2$  modified with platinum (IV) chloride complexes also showed bacterial inactivation under visible light [31]. The bactericidal action was associated with generation of superoxide radicals ( $\text{O}_2^{\bullet-}$ ) produced by reduction of molecular oxygen by the  $\text{TiO}_2$  conduction band electrons ( $e_{\text{CB}}^-$ ). In contact with water molecules these radicals, in turn, disproportionate, thus generating  $\text{H}_2\text{O}_2$ . The hydrogen peroxide can act as an irreversible electron acceptor leading the formation of  $\cdot\text{OH}$  radicals.

We hereby present the photocatalytic activity of a custom N- and S-doped commercial anatase powder, Tayca TKP 102, towards the *E. coli* inactivation and phenol and DCA oxidation under UV and visible light. ESR experiments using DMPO as a spin trap of hydroxyl/superoxide ( $\cdot\text{OH}/\text{O}_2^{\bullet-}$ ) radicals and TMP-OH as singlet oxygen ( $^1\text{O}_2$ ) quencher were carried out separately to detect ROS generated under UV and visible light illuminations, respectively.

## 2. Experimental

### 2.1. Materials

Tayca Corporation kindly supplied commercial  $\text{TiO}_2$  nanoparticles TKP 102 (96% anatase, primary crystallite particle size of 15 nm). Phenol, dichloroacetate (DCA) (99% Fluka chemicals) and thiourea (99% Sigma-Aldrich) were used as received.

### 2.2. Preparation of doped Tayca TKP 102

The powder of N- and S-doped  $\text{TiO}_2$  was prepared by mechanical mixing of thiourea with TKP 102  $\text{TiO}_2$  sample in a 4:1 (w/w) ratio. The material was annealed under air atmosphere during 1 h at 400 °C with a heating rate of 10 °C for minute and then cooled at room temperature. After heating the materials were washed with Milli-Q water three times, dried at 70 °C and then crushed in an agate mortar into a fine powder before use.

### 2.3. Powder characterization

#### 2.3.1. Diffuse reflectance spectroscopy (DRS)

DRS spectra of  $\text{TiO}_2$  powders were measured with a Varian Cary 1E spectrophotometer equipped with a diffuse reflectance accessory.

#### 2.3.2. X-ray photoelectron spectroscopy (XPS)

XPS analyses were carried out on a XPS Analyzer Kratos model Axis Ultra with a monochromatic Al  $\text{K}\alpha$  and charge neutralizer.

The deconvolution software program was provided by Kratos. This software is the standard program used and is accepted as reference in the field.

All the binding energies were referenced to the C 1s peak at 285 eV of carbon. Powder samples were prepared by deposition of catalyst on carbon type stuck to sample holder. The powder samples were analyzed with very large spot with dimension 0.3 mm × 0.7 mm. Therefore, it was assumed that the recorded spectrum is characteristic of "average" particles. Using a large spot the signal/noise ratio was improved significantly. The atomic concentrations were determined with an increased sensitivity factor because in general the signal/noise ratio observed was weak. This analysis was carried out: (a) taking a larger area (b) the signal accumulation time was increased and (c) the elements analyzed like N did not have a weak sensitivity. The detection limit was not 0.1 at.% but 0.03 at%.

#### 2.3.3. Specific surface area (SSA)

Specific surface areas (SSA) was measured using nitrogen adsorption-desorption at 77 K via a Sorptomatic 1990 instrument (Carlo Erba) and calculated using the Brunauer–Emmett–Teller (BET) method.

### 2.3.4. ESR reactive scavenging of ROS

**2.3.4.1. Sample preparation for ESR detection of hydroxyl and superoxide radicals.** For ESR spin trapping of hydroxyl and superoxide radicals 3.2 mg of N- and S-doped nano $\text{TiO}_2$  powder was dispersed in 10 mL of ultrapure water (Millipore, Simplicity UV, Millipore Corp., France). The water suspension of  $\text{TiO}_2$  nanoparticles was then homogenized for 10 min in an ultra-sound bath.

The standard commercially available spin trap, 5,5'-dimethyl-pyrroline-1-oxide (DMPO), from Sigma was used for ESR detection of hydroxyl and superoxide radicals. Before application, DMPO was carefully purified by filtration on charcoal. The obtained stock solution of 0.5 M DMPO in ultrapure water was stored at –20 °C. Immediately before performing ESR measurements, the water suspension of N- and S-doped  $\text{TiO}_2$  nanoparticles was mixed with the stock solution of DMPO to achieve the final spin trap concentration of 100 mM. Subsequently, the 1 mL aliquot of prepared suspensions containing DMPO and N- and S-doped nano $\text{TiO}_2$  was transferred into small (5 mL volume, 20 mm OD and 30 mm height) Pyrex beaker and exposed to UV-A illumination (wavelength ~365 nm) using a UV spot light source, Lightingcure™, model LC-8, from Hamamatsu Photonics, France. The

Lightningcure<sup>TM</sup> source incorporates a 200W Mercury-Xenon lamp (model L7212-01) and a quartz fiber light guide, which is optimized for high transmittance in the UV spectral region. The light guide termination was positioned at 0.5 cm distance over the open face of the beaker, thus yielding illumination power density of 10 mW/cm<sup>2</sup> (for the lamp power setting at 20%). The intensity of UV-A light illuminating the aqueous suspension of N- and S-doped nanoTiO<sub>2</sub> was measured with a UV-meter, model C6080, from Hamamatsu Photonic, France. To avoid sedimentation during illumination, the suspension of nanoTiO<sub>2</sub> was constantly stirred with the use of a small magnetic stirrer.

**2.3.4.2. Sample preparation for ESR scavenging of singlet oxygen.** For ESR reactive scavenging of singlet oxygen 3.2 mg of N- and S-doped nanoTiO<sub>2</sub> powder was suspended in 10 mL of either ultrapure H<sub>2</sub>O or D<sub>2</sub>O (99.9% atomic purity from Aldrich). The diamagnetic singlet oxygen-scavenging reagent, 2,2,6,6-tetramethyl-4-piperidinol (TMP-OH) from Fluka was used as received to detect light-induced singlet oxygen formation in the aqueous (H<sub>2</sub>O and D<sub>2</sub>O) suspensions of N- and S-doped TiO<sub>2</sub>. TMP-OH reacts with singlet oxygen, thus yielding a paramagnetic product, 4-hydroxy-2,2,6,6-tetramethylpiperidine 1-oxyl (TEMPOL). This approach, firstly introduced by Lion et al. [33], is thought to be highly specific to the formation of singlet oxygen [34]. The final concentration of TMP-OH in aqueous suspensions of TiO<sub>2</sub> nanoparticles was adjusted to 2.5 mM. 1 mL aliquot of such prepared suspension was then transferred into a 5 mL Pyrex beaker and exposed to illumination with the white light from a spot white light source (150 W halogen lamp, Model 6000, Intralux, Switzerland). Similarly to the above-described procedure of the sample illumination with UV-A, the aqueous suspensions exposed to the visible light were also magnetically stirred.

**2.3.4.3. ESR detection of spin-trapped ROS and reactively scavenged singlet oxygen.** Immediately after subsequent exposures to UV-A or white light illuminations, aliquots of ca. 7  $\mu$ L of illuminated suspensions were transferred into 0.7 mm ID and 0.87 mm OD quartz capillary tubes from VitroCom, NJ, USA (sample height of 25 mm) and sealed on both ends with Cha-Seal<sup>TM</sup> tube sealing compound (Medex International, Inc., USA).

ESR experiments were carried out at room temperature using an ESP300E spectrometer (Bruker BioSpin GmbH), equipped with a standard rectangular mode TE<sub>102</sub> cavity. Routinely, for each experimental point, five-scan field-swept ESR spectra were recorded. The typical instrumental setting were: microwave frequency 9.38 GHz, microwave power 2.0 mW, sweep width 120 G, modulation frequency 100 kHz, modulation amplitude 0.5 G, receiver gain  $4 \times 10^4$ , time constant 20.48 ms, conversion time 40.96 ms, and time per single scan 41.9 s.

#### 2.4. Photocatalytic activity

Cylindrical Pyrex bottles (50 mL) were used, a TiO<sub>2</sub> concentration of 1.0 mg mL<sup>-1</sup> was selected and oxygen (present in the air) was the electron acceptor. The suspension was kept under magnetic stirring and illuminated by 5 Black light lamps Phillips TLD 18 W (emission spectra: 330–400 nm and UV intensity between 300 and 400 nm: 38 W m<sup>-2</sup>) and 5 fluorescent lamps Phillips TLD-18W blue (emission spectra: 400–500 nm, UV intensity: 0.1 W m<sup>-2</sup> and intensity between 290 and 1100 nm: 60 W m<sup>-2</sup>). The radiant flux was monitored with a Kipp & Zonen (CM3) power meter (Omni instruments Ltd., Dundee, UK). Temperature of the experiments was never superior to 38 °C. Samples were periodically collected to follow the reaction kinetics. Results represent the average of three experimental runs and their standard deviations were equal or lower than 15% for the

microbiological analysis and less of 8% for HPLC and UV spectroscopic analysis.

#### 2.4.1. Bacterial inactivation

Photocatalytic bactericidal activity was measured by sampling *Escherichia coli* (*E. coli*) strain K12 MG 1655 from the photoreactor. Before the experiment, bacteria were inoculated into nutrient broth (Oxoid No. 2, Switzerland) and grown overnight at 37 °C. During the stationary growth phase, bacteria cells were harvested by centrifugation at 5000 RPM for 10 min at 4 °C. The bacterial pellet was then washed three times with a saline solution (8 mg mL<sup>-1</sup> NaCl and 0.8 mg mL<sup>-1</sup> KCl in Milli-Q water, pH 7 by addition of HCl or NaOH). A suitable cell concentration (10<sup>4</sup> colony forming units (CFU) per mL<sup>-1</sup>) was inoculated in the reactor's saline solution. Then, the inoculated Pyrex bottles with the catalyst added were illuminated during 2 h and samples (1.0 mL) were taken at different time intervals. Serial dilutions were performed in saline solution and 100  $\mu$ L volumes were inoculated in a plate count agar (PCA, Merck, Germany) growth medium. The number of colonies was counted 24 h after inoculation at 37 °C. Control experiments (*E. coli* and UV or visible light without catalyst) and (*E. coli* + catalyst without light) were also performed.

#### 2.4.2. Phenol photocatalytic oxidation

The procedure was the same used in the *E. coli* inactivation. Phenol solution containing  $1 \times 10^{-4}$  M was added to the Pyrex glass reactors. Samples were taken and filtered by 0.2  $\mu$ m membranes. Phenol oxidation was followed by HPLC (Hewlett-Packard series 1100) and with a reverse phase Spherisorb silica column (Macherey-Nagel). As mobile phase was used acetonitrile:water (60:40). Phenol and p-benzoquinone detection was carried out by Diode Array Detector (DAD) at 220 and 244 nm, respectively.

#### 2.4.3. Dichloroacetate (DCA) photocatalytic oxidation

DCA solution containing  $1 \times 10^{-3}$  M was added to the Pyrex glass reactors. Samples were taken and filtered by 0.2  $\mu$ m (micrometer) membranes. DCA oxidation was followed by HPLC (Hewlett-Packard series 1100) analysis using a column Supelcogel H Supelco at 60 °C and a H<sub>2</sub>SO<sub>4</sub> solution  $5 \times 10^{-3}$  M was used as mobile phase. Detection was done by DAD detector at 210 nm.

#### 2.4.4. Tetranitromethane (TNM) experiments

TNM solution containing  $1 \times 10^{-2}$  M was added to the Pyrex glass reactor and the reduction by e<sub>CB</sub><sup>-</sup> or O<sub>2</sub><sup>-</sup> producing the anion C(NO<sub>2</sub>)<sub>3</sub><sup>-</sup> was followed by UV-spectroscopy at 350 nm.

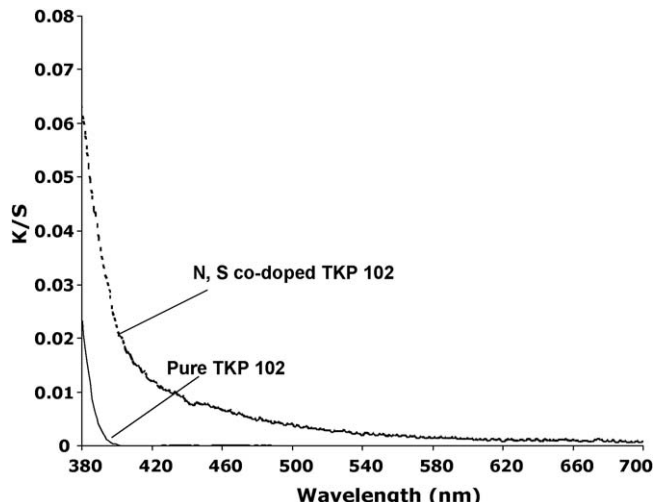


Fig. 1. DRS spectra of pure TKP 102 and TKP 102 treated with thiourea at 400 °C.

### 3. Results and discussion

#### 3.1. Characterization of doped $TiO_2$ TKP 102

Fig. 1 shows the DRS spectra of pure TKP 102 and doped TKP 102 treated with thiourea and annealed at 400 °C. Pure material presents the typical absorption of anatase  $TiO_2$  at wavelengths below 400 nm. Pure powder annealed at 400 °C did not show any alteration in its DRS spectrum (data not showed). In contrast, TKP 102 powders treated with thiourea showed the typical absorption of anatase  $TiO_2$  ( $\lambda < 400$  nm) but also a marked absorption shoulder in the visible region (between 400 and 550 nm). In a previous work published by our group [16], the band gap of this material was estimated to be of 2.85 eV using the Kubelka–Munk function.

Fig. 2 shows the XPS measurements to identify the species responsible for the visible absorption. Pure TKP 102 did not reveal

presence of N, and S impurities. In contrast, the characteristic XPS peaks of N 1s, S 2p and C 1s were found in the doped TKP 102.

In particular, the XPS spectra revealed the presence of two N 1s peaks at binding energies (BE) of 399.2 and 400.7 eV. The assignation of N 1s peaks in N-doped  $TiO_2$  by XPS remains a controversial issue. N 1s peak found at BE around 397 eV have been often assigned as substitutional N-doping (Ti–N bond) [10,17,35–37], while N 1s peaks at BE > 399 eV have been assigned to interstitial N-doping (Ti–O–N species) [38,39]. Thus, the peak at BE of 399.2 and 400.7 eV found in these study (Fig. 2) can be assigned to interstitial N-doping and/or the formation of Ti–O–N species.

The S 2p peaks characteristic for the presence of sulfur atoms are found for the highest oxidation states (such as  $SO_4^{2-}$ ) at binding energies >168 eV. The peaks between 163 and 166 eV are due to presence of  $SO_3^{2-}$  species [40]. Other two peaks often related to S-doping were found at 162.8 and 167.2 eV due to

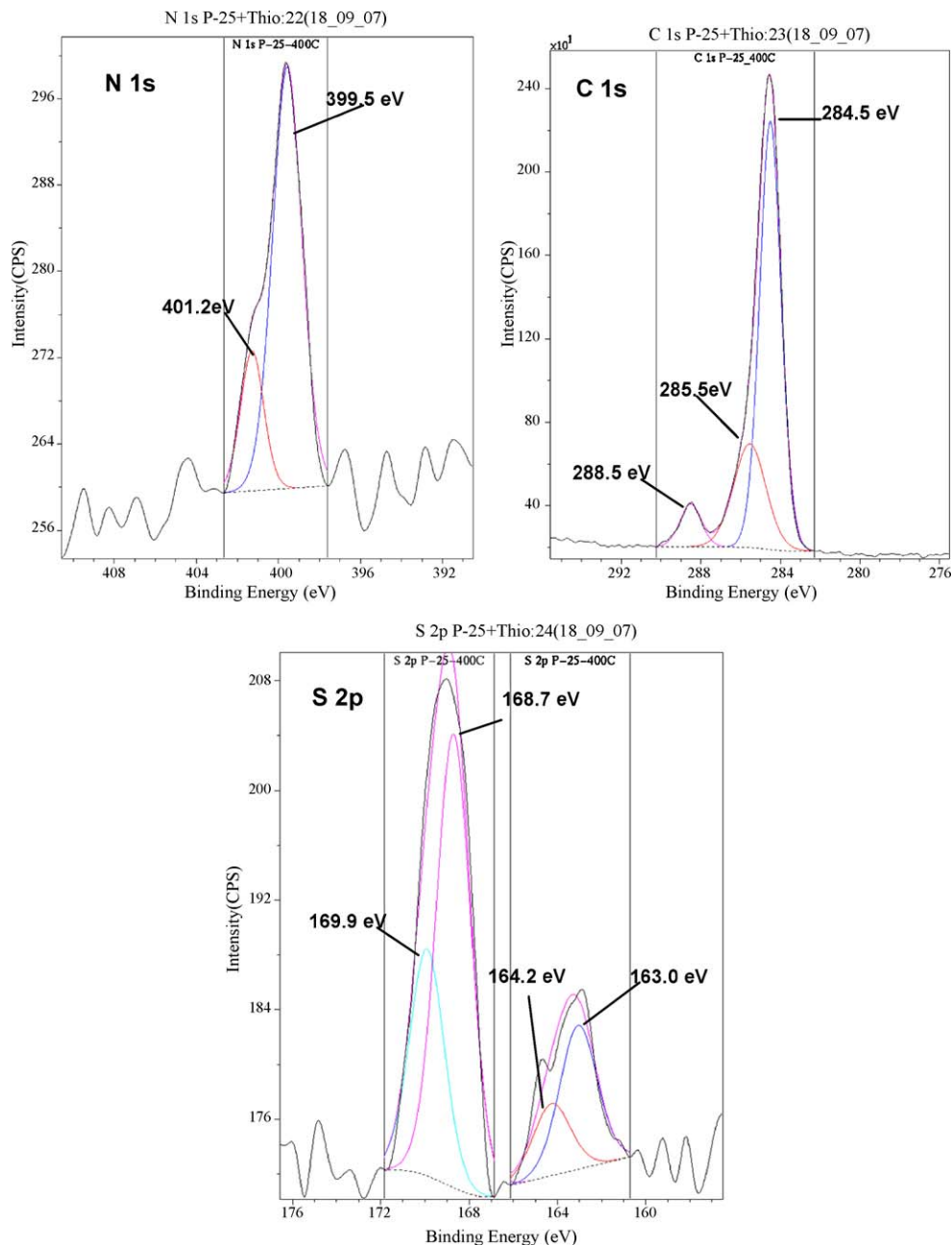


Fig. 2. N 1s, C 1s and S 2p XPS peaks acquired for N, S co-doped TKP 102 powder annealed at 400 °C.

anionic S species [11,24,41–43] cationic S species [11,26], respectively.

The C 1s peak revealed adventitious carbon at 284 eV due to sample contamination. It has been reported that the anionic C-doping leading to visible absorption shows a C 1s peak at 282 eV [44], but this peak was not found in our samples. Carbonate peaks assigned to C–O and C=O bonds were found at binding energies around 286.6 and 288.6 eV, respectively. These findings reveals that carbonaceous species formed during the annealing of TiO<sub>2</sub> powder treated with thiourea do not participate in the absorption of visible light.

BET specific surface area (SSA) of pure and pure annealed TKP 102 were 110 and 84.2 m<sup>2</sup> g<sup>-1</sup>, respectively, while the powder annealed at 400 °C in the presence of thiourea showed SSA of 79.5 m<sup>2</sup> g<sup>-1</sup>. The decreasing of SSA in doped powder was due to particle sintering.

In summary, commercial TKP 102 powder treated with thiourea and annealed at 400 °C showed visible absorption due to N, S co-doping leading to interstitial N-doping and anionic and cationic S-doping. Both types of doping might generate localized N or S midgap levels. From these midgap states the electronic promotion may be produced by visible light absorption (Scheme 1).

### 3.2. Photocatalytic activity under UV light illumination

#### 3.2.1. Photocatalytic oxidation of phenol

Fig. 3 shows that under UV light pure and N, S co-doped TiO<sub>2</sub> retains its photocatalytic activity after annealing at 400 °C. Fig. 4a and b shows the HPLC chromatograms taken at 244 nm at time 0 and 60 min of water containing phenol and treated with pure and N, S co-doped TKP 102, respectively. At 0 min, it is only noted one peak with a retention time at 3.8 min corresponding to phenol. After 60 min, this peak decreased and a new peak appeared with the retention time of 3.6 min corresponding to p-benzoquinone. p-benzoquinone seems to be a by-product in the first step of phenol degradation with both powders. Many authors [45–48] have mentioned that the first step in the phenol degradation on TiO<sub>2</sub> is the electrophilic attack of the •OH radicals on the aromatic moiety producing hydroquinone or p-benzoquinone. Phenol was not affected by the decreasing of specific surface area because it does not need to be adsorbed on the TiO<sub>2</sub> surface to undergo the attack by •OH radicals leading to its decomposition [50].

#### 3.2.2. Photocatalytic oxidation of dichloroacetate (DCA)

Fig. 5 shows that bare UV light did not affect the DCA. The photocatalytic DCA decomposition rate was affected by the TiO<sub>2</sub> annealing temperature. It is customarily accepted that, after adsorption on the TiO<sub>2</sub> surface, DCA oxidation occurs due to photo-produced holes (h<sub>VB</sub><sup>+</sup>) in the TiO<sub>2</sub> valence band [49,50]. This adsorption is favored at pH 3.0, since the TiO<sub>2</sub> surface is positively

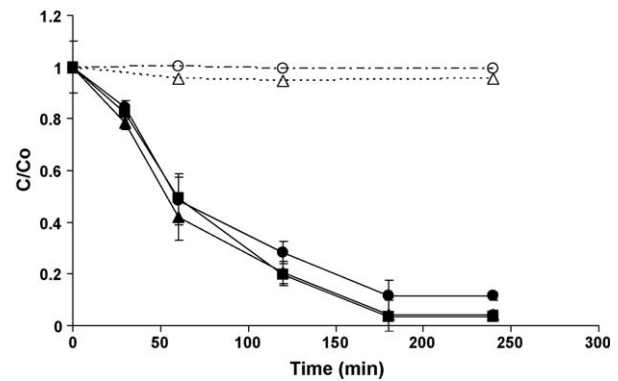


Fig. 3. Photocatalytic oxidation of phenol under UV light. (▲) N, S co-doped TKP 102 annealed at 400 °C. (●) Pure TKP 102. (■) Pure TKP 102 annealed at 400 °C. (○) Pure TKP 102 without light. (△) N, S co-doped TKP 102 annealed at 400 °C without light. Experimental conditions: pH 6.0, UV intensity 30 W m<sup>-2</sup> and concentration of N, S TiO<sub>2</sub> of 1 g L<sup>-1</sup>.

charged (pH<sub>pzc</sub> for anatase TiO<sub>2</sub> is 6.0) and most of DCA molecules are in the deprotonated form (Cl<sub>2</sub>CHCOO<sup>-</sup>), their pK<sub>a</sub> being of 1.8.

#### 3.2.3. Photocatalytic *E. coli* inactivation

Bare UV light did not lead to *E. coli* inactivation, nor did pure or doped TKP 102 in the dark. In contrast, *E. coli* inactivation was achieved under UV illumination in the presence of either doped or pure TKP powders (Fig. 6).

As shown in Fig. 6, annealing of the pure or doped TKP 102 powders impaired the photocatalytic activity under UV light. In our previous work [16], we demonstrated that the annealing process leads to de-hydroxylation of the TKP 102 surface, thus affecting negatively the *E. coli* inactivation.

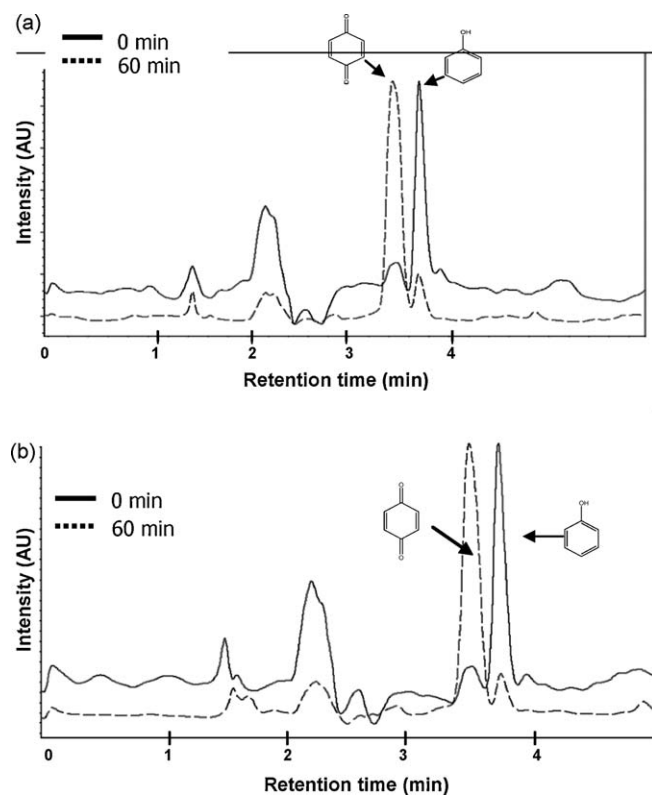
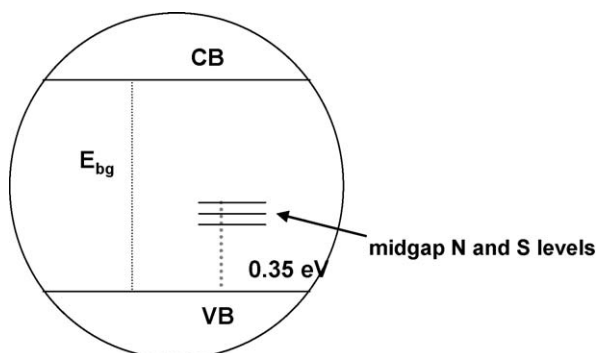
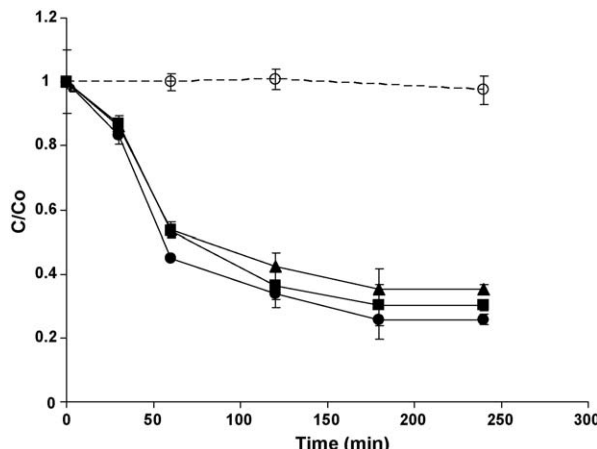


Fig. 4. Chromatograms using DAD detector at 244 nm revealing the formation of p-benzoquinone upon UV light (a) pure TKP 102 and (b) N, S co-doped TKP 102.



Scheme 1. Localization of N- and S-related isolated levels states in the band gap of N, S co-doped TiO<sub>2</sub>.



**Fig. 5.** Photocatalytic oxidation of dichloroacetic acid (DCA) under UV light. (▲) N, S co-doped TKP 102 annealed at 400 °C. (●) Pure TKP 102. (■) Pure TKP 102 annealed at 400 °C. (○) Pure TKP 102 without light. (△) N, S co-doped TKP 102 annealed at 400 °C without light. pH: 3.0. UV intensity: 30 W m<sup>2</sup> [TiO<sub>2</sub>]: 1 g L<sup>-1</sup>.

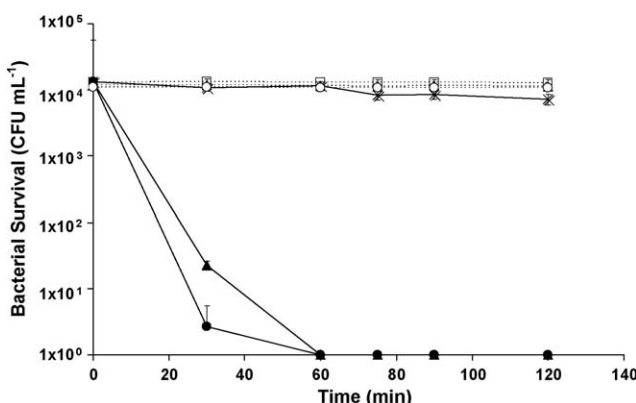


**Fig. 6.** Photocatalytic *E. coli* inactivation under UV light. (▲) N, S co-doped TKP 102 annealed at 400 °C and pure TKP 102 annealed at 400 °C (an average was taken in account since their activities were similar). (●) Pure TKP 102. (○) Pure TKP 102 without light. (△) N, S co-doped TKP 102 annealed at 400 °C without light. (□) Pure TKP 102 annealed at 400 °C without light. (\*) *E. coli* under UV light irradiation without catalyst. pH: 7.0. UV intensity: 30 W m<sup>2</sup> [TiO<sub>2</sub>]: 1 g L<sup>-1</sup>.

### 3.2.4. ESR spin-trapping experiments under UV light

The nitroxyl spin trap 5,5-dimethyl-1-pyrroline *N*-oxide (DMPO) is widely used to provide evidence for the involvement of free radicals in many chemical and biological reactions [51]. In particular, DMPO reacts with  $\cdot\text{OH}$  and  $\text{O}_2^{\cdot-}$  radicals, thus leading to

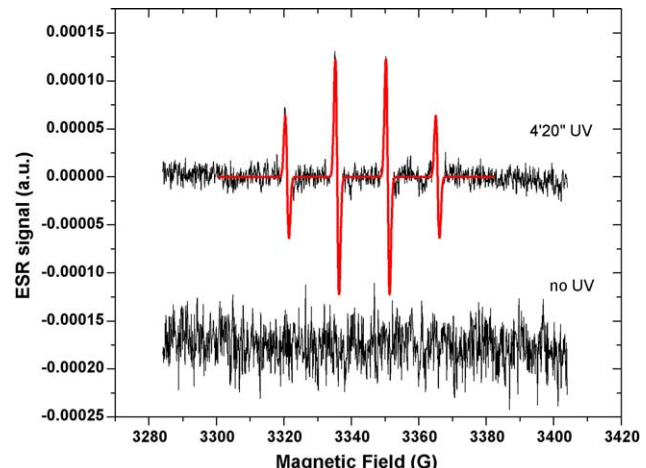


**Fig. 7.** ESR spectrum of DMPO- $\cdot\text{OH}$  adduct observed after 4 min 20 s of UV-A illumination ( $\lambda = 365$  nm, 10 mW/cm<sup>2</sup>) for ROS reactive spin trapping with DMPO in the presence of N, S co-doped TKP 102.

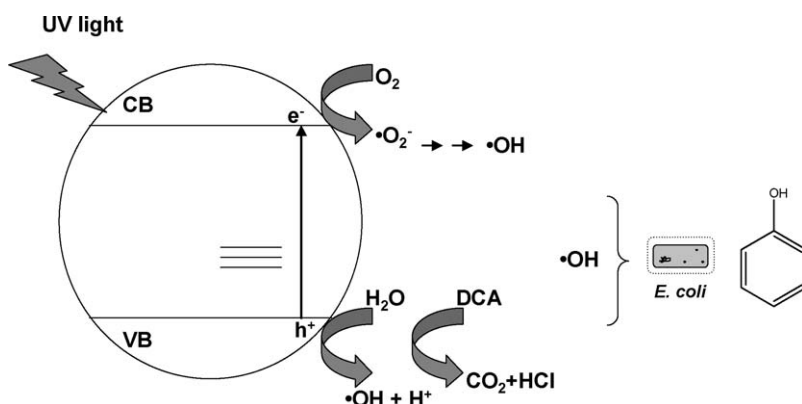
the formation of adducts, DMPO-OH and DMPO-OOH, respectively. Both resulting products are paramagnetic and can easily be detected by ESR. We used ESR spin trapping with DMPO to detect formation of  $\cdot\text{OH}$  and  $\text{O}_2^{\cdot-}$  radicals, under illumination of pure and N- and S-doped nanoTiO<sub>2</sub> with both visible and UV light.

ESR reactive spin trapping of ROS (Fig. 7) revealed the presence of the characteristic 1:2:2:1 quartet signal of DMPO- $\cdot\text{OH}$  adduct only when N, S co-doped powder was exposed to UV light. It was also found the signal of DMPO- $\cdot\text{OH}$  adduct when undoped TiO<sub>2</sub> TKP 102 was illuminated with UV light (dates not showed). This points to a classical mechanism of the UV-light-induced promotion of valence band electrons to the conduction band, which yields valence band holes ( $\text{h}_{\text{VB}}^+$ ) and produces  $\cdot\text{OH}$  radicals at the particle surface. The latter process is implicated in the photocatalytic decomposition of DCA, phenol oxidation and *E. coli* inactivation, respectively (Scheme 2). These findings are also in agreement with recent observations by Fu et al. [25].

### 3.3. Photocatalytic activity under visible light illumination

#### 3.3.1. Photocatalytic treatment of phenol and DCA

When visible light (wavelength between 400 and 500 nm) was used, the phenol decreased weakly in the presence of the pure and N, S co-doped TiO<sub>2</sub> photocatalyst (Fig. 8). Pure TiO<sub>2</sub> generates some ROS that are responsible for phenol degradation. However, an alternative explanation is given by Kim and Choi [52], reporting



**Scheme 2.** Mechanism of the photocatalytic action for N, S co-doped TiO<sub>2</sub> exposed to UV light.

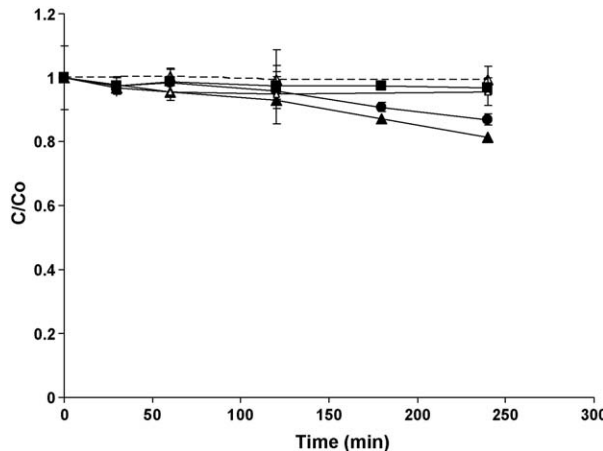


**Fig. 8.** Photocatalytic oxidation of phenol under visible light. (▲) N, S co-doped TKP 102 annealed at 400 °C. (●) Pure TKP 102. (■) Pure TKP 102 annealed at 400 °C. (○) Pure TKP 102 without light. (△) N, S co-doped TKP 102 annealed at 400 °C without light. pH: 6.0. Total light Intensity: 60 W m<sup>-2</sup> and UV intensity: 0.1 W m<sup>-2</sup>, [TiO<sub>2</sub>]: 1 g L<sup>-1</sup>.

phenol oxidation on pure TiO<sub>2</sub> under visible light through a surface complexation mechanism. They suggested that visible light-induced electron transfer from phenolic substances to the TiO<sub>2</sub> conduction band is feasible.

DCA concentration was not affected when visible light was used either in undoped or co-doped N, S TiO<sub>2</sub> (data not showed).

### 3.3.2. Photocatalytic *E. coli* inactivation under visible light

*E. coli* inactivation was observed to proceed more favorably in N, S doped TiO<sub>2</sub> nanoparticles than in pure TKP 102 powders (Fig. 9).

Under visible light illumination, pure TKP 102 powder revealed some activity towards *E. coli* inactivation probably due to stimulation at wavelengths below 400 nm, since a small portion of available light was also emitted at these wavelengths by the used visible light sources.

It is also worth mentioning that in this study the initial bacterial concentration was very low (of 10<sup>4</sup> CFU mL<sup>-1</sup>). Clearly, under such low cell concentration, even a moderate generation of ROS will

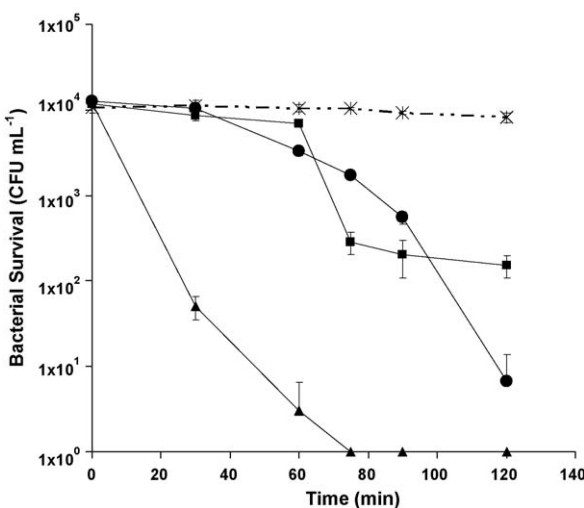


**Fig. 9.** Photocatalytic *E. coli* inactivation under visible light. (▲) N, S co-doped TKP 102 annealed at 400 °C. (●) Pure TKP 102. (■) Pure TKP 102 annealed at 400 °C. *E. coli* under visible illumination without catalyst. pH: 7.0. Total light Intensity: 60 W m<sup>-2</sup> and UV intensity: 0.1 W m<sup>-2</sup>, [TiO<sub>2</sub>]: 1 g L<sup>-1</sup>.

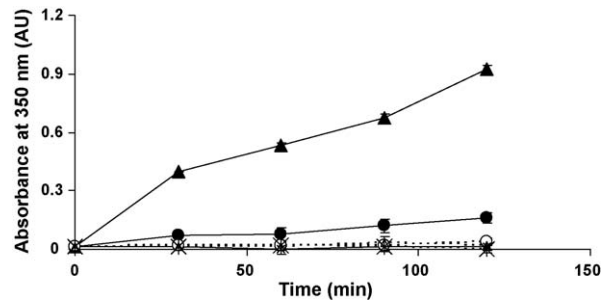


**Fig. 10.** Tetranitromethane (TNM) reduction by pure and N, S co-doped TKP 102 under visible illumination. (▲) N, S co-doped TKP 102-400 °C. (●) undoped TKP 102. (△) TNM + N, S co-doped TKP 102-400 °C without light. (○) Pure TKP 102 without light. (\*) TNM only visible light. pH: 6.0. Total light Intensity: 60 W m<sup>-2</sup> and UV intensity: 0.1 W m<sup>-2</sup>, [TiO<sub>2</sub>]: 1 g L<sup>-1</sup>.

reveal its influence on *E. coli* population, especially in a logarithmic representation.

When pure and annealed TiO<sub>2</sub> was used, an initial lag phase was observed [31,53]. This phenomenon might be understood in terms of a self-defense mechanism that bacteria activate against ROS. This mechanism prevails until the ROS-mediated damage caused to bacterial cells overcomes the self-defense or auto-repairing processes. In contrast, in the case of N, S doped nanoTiO<sub>2</sub>, the

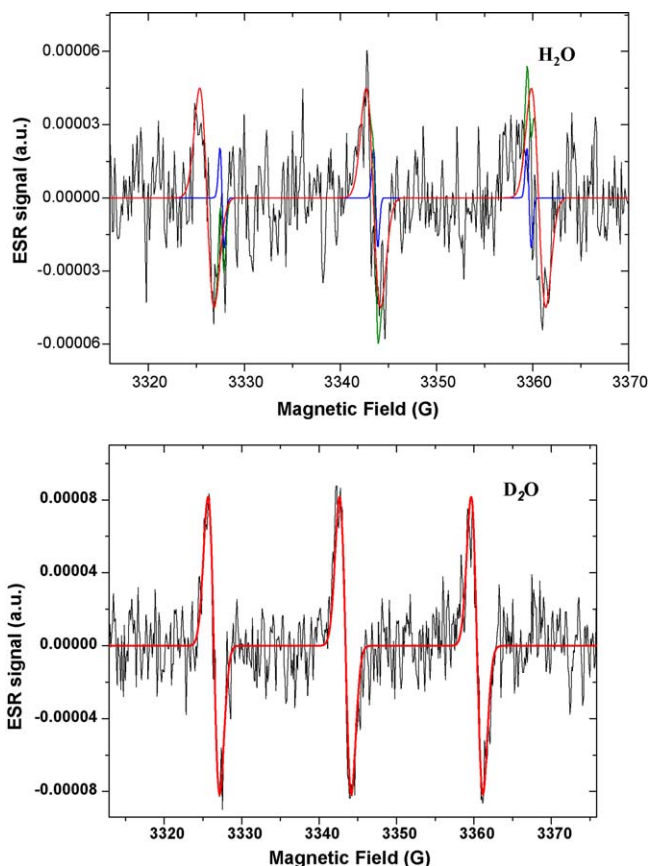
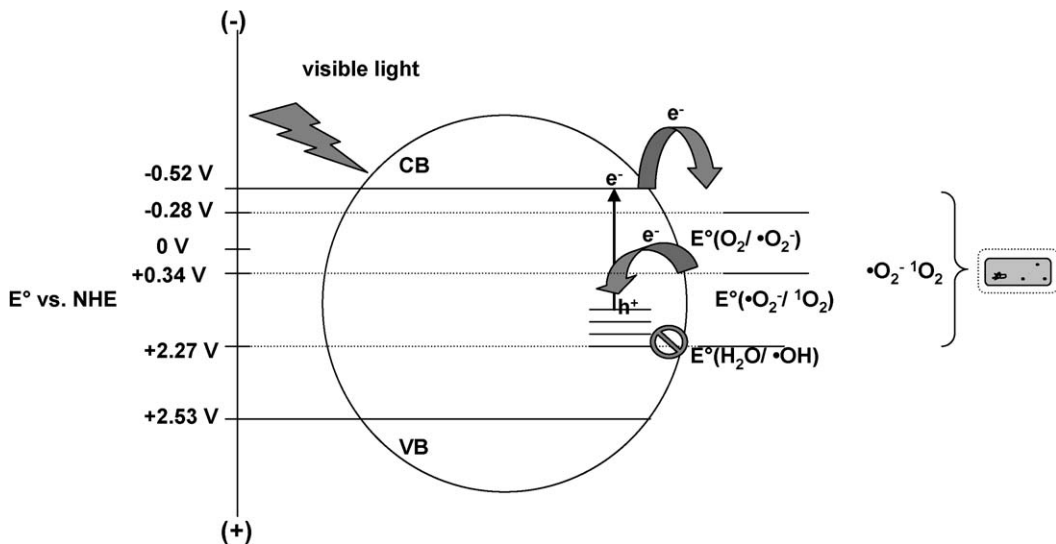


**Fig. 11.** ESR spectra of TEMPOL observed after 16 min of illumination with visible light of the aqueous suspensions of N, S co-doped nanoTiO<sub>2</sub> in the presence of 2.5 mM concentration of singlet oxygen scavenger, TMP-OH. Upper panel: ESR trace recorded in H<sub>2</sub>O. Lower panel: ESR trace recorded in D<sub>2</sub>O. Red solid line corresponds to a simulative fit of the ESR spectrum of TEMPOL ( $A_{iso} = 17.4$  G). (For interpretation of the references to color in this figure legend, the reader is referred to the web version of the article.)



**Scheme 3.** Possible mechanism for the photocatalytic action of N, S co-doped TiO<sub>2</sub> exposed to visible light, including singlet oxygen photo-generation.

formation of ROS was stronger from the beginning of exposure to visible light and no initial lag phase was observed.

### 3.3.3. Tetranitromethane (TNM) reduction experiments and singlet oxygen detection by ESR under visible light

It is well known that on the surface of TiO<sub>2</sub> nanoparticles, tetranitromethane (TNM) can react with the electron promoted to the conduction band and/or with superoxide radical (O<sub>2</sub><sup>•-</sup>) ( $k = 2 \times 10^9 \text{ M}^{-1} \text{ s}^{-1}$ ). This process yields nitroform anions which strongly absorb at 350 nm ( $\epsilon = 15,000 \text{ M}^{-1} \text{ cm}^{-1}$ ) [54,55].

Fig. 10 shows the results of TNM reduction under visible light irradiation. Dark experiments and visible light irradiation of TNM solutions in absence of TiO<sub>2</sub> did not reveal nitroform anion production. However, a slight reduction of TNM by pure TKP 102 powder was observed under visible light. This might point to a weak formation of e<sup>-</sup>/h<sup>+</sup> pairs under visible light illumination. Consequently, it would result in rather low ROS concentrations and might account for a poor photocatalytic activity of TKP 102 towards *E. coli* inactivation and phenol oxidation. In contrast, when N, S co-doped TiO<sub>2</sub> was illuminated with visible light in presence of TNM, a strong production of nitroform anion was observed, giving evidence for the existence of electronic promotion by visible light.

On the other hand, ESR spin trapping using DMPO as hydroxyl radical scavenger did not detect DMPO-OH adduct (data not showed), when N, S co-doped TKP 102 powder was irradiated with visible light. Therefore, to find other reactive oxygen species, we also performed ESR detection using singlet oxygen quencher, TMP-OH. TMP-OH reacts with singlet oxygen thus forming the paramagnetic product, TEMPOL, which can easily be followed by ESR detection [56]. Singlet oxygen formation was clearly evidenced by observation of a characteristic 1:1:1 triplet signal of TEMPOL (Fig. 11). Moreover, as expected for singlet oxygen mediated processes, the ESR signal intensity of TEMPOL was markedly enhanced when D<sub>2</sub>O was used as solvent [57,58]. Konaka et al. reported a very similar isotopic enhancement of the ESR-detected singlet oxygen for TiO<sub>2</sub> nanoparticles suspended in deuterium oxide [56]. Recently, the formation of reactive singlet oxygen molecules in the photocatalytic TiO<sub>2</sub> aqueous suspension systems has also been evidenced by a direct detection of the singlet oxygen-related near-infrared phosphorescence at 1270 nm [59]. Formation of singlet oxygen has also been reported for surfaces coated with undoped TiO<sub>2</sub> under UV illumination in aqueous media [60–62], as

well as for N-doped TiO<sub>2</sub> coatings upon visible irradiation in gas phase [63]. The mechanism of <sup>1</sup>O<sub>2</sub> photosensitization by TiO<sub>2</sub> nanoparticles is closely related to the formation of superoxide radicals (O<sub>2</sub><sup>•-</sup>) due to dioxygen reduction by solvated e<sub>CB</sub><sup>-</sup> [62]. Thus formed O<sub>2</sub><sup>•-</sup> species can undergo a further oxidation to form singlet oxygen. This oxidation is thermodynamically favored as  $E^\circ(O_2^{\bullet-}/^1O_2) = 0.34 \text{ V vs. NHE}$  [64].

This is probably due to the photo-excitation of electrons from localized midgap N or S levels to the conduction band generating localized hole on N or S levels. Reduction of dioxygen by e<sub>CB</sub><sup>-</sup> is thermodynamically favored producing superoxide radical ( $E^\circ(O_2/O_2^{\bullet-}) = -0.28 \text{ V vs. NHE}$  at pH 7 [65]). It has been demonstrated that the redox potential of conduction band is not modified by non-metallic doping [27]. In contrast with doped TiO<sub>2</sub>, OH<sup>-</sup> ions (from water) and DCA could not be oxidized due to the potentials involved ( $E^\circ(H_2O/OH^{\bullet-}) = +2.27 \text{ V vs. NHE}$  at pH 7 [65]). Probably the hole produced by visible light has not the required positive potential to generate OH radicals or to directly oxidize DCA. However, as the superoxide radical oxidation can lead to <sup>1</sup>O<sub>2</sub> (Scheme 3), O<sub>2</sub><sup>•-</sup> and <sup>1</sup>O<sub>2</sub>, which are toxic to microorganisms [66,67], are probably responsible for the *E. coli* abatement under visible light. In addition, Hirakawa and Hirano [60] showed that generation of <sup>1</sup>O<sub>2</sub> on TiO<sub>2</sub> surfaces could be enhanced in the microenvironment of the phospholipid membrane yielding lipid peroxidation reactions and provoking the cell abatement. Singlet oxygen formation could also explain the weak phenol degradation obtained under visible irradiation when N, S TKP 102 was used. The literature reports as possible the phenol attack by singlet oxygen, but this reaction would be only favored at basic pH [68].

## 4. Conclusions

The commercial Tayca TKP 102 anatase TiO<sub>2</sub> nanopowder was mechanically mixed with thiourea and annealed at 400 °C during 1 h. Thus obtained material was found to be N, S co-doped TiO<sub>2</sub> nanopowder and revealed a marked photocatalytic activity under visible light illumination.

Firstly, the photocatalytic properties of N, S co-doped TiO<sub>2</sub> were checked under UV illumination. The doped material revealed the strong photocatalytic activity towards the photo-degradation of phenol and DCA, as well as inactivation of *E. coli* under exposure to UV light. ESR spin-trapping experiments using DMPO, revealed

that the main oxidative species photo-produced under UV illumination responsible of phenol oxidation and *E. coli* inactivation were  $\cdot\text{OH}$  radicals, while DCA was degraded directly by  $\text{h}_{\text{VB}}^+$ .

In contrast, when N, S co-doped  $\text{TiO}_2$  nanopowder was exposed to visible light, DCA was not degraded, phenol only partially decayed, while *E. coli* suffered fast inactivation.

Tetra-nitromethane (TNM) was strongly reduced with this doped material under visible light, most probably by the conduction band electrons ( $e_{\text{CB}}$ ) promoted from the localized N and/or S levels in the  $\text{TiO}_2$  band gap. Then, ESR experiments using the spin-trap, DMPO, showed that the oxidative potential of the visible light-induced holes populating the localized N and/or S states within the  $\text{TiO}_2$  band gap is not high enough to produce  $\cdot\text{OH}$  radicals or directly oxidize DCA molecules. In contrast, the ESR experiments with singlet oxygen quencher, TMP-OH, revealed the formation of singlet oxygen under visible light illumination of N, S co-doped  $\text{TiO}_2$ .

Thus, we report here the first evidence for the  ${}^1\text{O}_2$  formation upon visible light irradiation of N- and S-doped  $\text{TiO}_2$  anatase nanoparticles in aqueous media. Moreover, our findings point to the presence and a marked toxicity of  ${}^1\text{O}_2$  and  $\cdot\text{O}_2^-$  generated under visible light illumination in aqueous suspensions of N, S  $\text{TiO}_2$  to microorganisms. In contrast, other ROS generated under such conditions seem to be only weakly active towards phenol degradation and were found totally innocuous to DCA. These results are significant with respect to a better understanding the photocatalytic mechanisms related to doped  $\text{TiO}_2$ . In particular, they point to the potential role of singlet oxygen as an intermediate in photo-oxidative degradation reactions stimulated by visible light in the presence of N, S co-doped  $\text{TiO}_2$  nanoparticles.

## Acknowledgements

The authors thank the Swiss Agency for Development and Cooperation and Cooperation@EPFL for its support to BIOSOLAR-DETOX project, Professor J-E. Moser and J. Teuscher from the Photochemical Dynamics Group (EPFL-Switzerland) for their help in the recording of DRS spectra, E. Casali for kindly recording the BET measurements and O. Masaaki from Tayca Corp (Japan) and S. Jansen from Mitsubishi Corp (Germany) for kindly supplied the samples of  $\text{TiO}_2$  powders Tayca. These studies were also partially supported by the Swiss National Science Foundation, project No. 205320 – 112164, "Biomolecules under stress: ESR in vitro study" (K.P., A.S., and L.F.).

## References

- [1] A. Fujishima, K. Honda, *Nature* 238 (1972) 37–38.
- [2] T.L. Thompson, J.T. Yates, *Chem. Rev.* 106 (2006) 4428–4453.
- [3] K. Hashimoto, H. Irie, A. Fujishima, *Jpn. J. Appl. Phys.* 44 (2005) 8269–8285.
- [4] A.V. Emeline, V.N. Kuznetsov, V.K. Rybchuk, N. Serpone, *Int. J. Photoenergy* (2008), doi:10.1155/2008/258394, 19 pp. (Article ID 258394).
- [5] W.Y. Choi, A. Termin, M.R. Hoffmann, *Angew. Chem.* 33 (1994) 1091–1092.
- [6] C. Burda, Y.B. Lou, X.B. Chen, A.C.S. Samia, J. Stout, J.L. Gole, *Nano Lett.* 3 (2003) 1049–1051.
- [7] M. Kitano, M. Matsuoka, M. Ueshima, M. Anpo, *Appl. Catal. A* 325 (2007) 1–14.
- [8] S. Sato, R. Nakamura, S. Abe, *Appl. Catal. A* 284 (2005) 131–137.
- [9] K. Kobayakawa, Y. Murakami, Y. Sato, *J. Photochem. Photobiol. A* 170 (2005) 177–179.
- [10] X. Chen, Y. Lou, A.C. Samia, C. Burda, J.L. Gole, *Adv. Funct. Mater.* 15 (2005) 41–49.
- [11] T. Ohno, M. Akiyoshi, T. Umebayashi, K. Asai, T. Mitsui, M. Matsamura, *Appl. Catal. A* 265 (2004) 115–121.
- [12] R. Silveyra, L. De la Torre Sáenz, W. Antúnez-Flores, V. Collins-Martínez, A. Aguilar-Elguézabal, *Catal. Today* 107/108 (2005) 602–605.
- [13] J.M. Gole, J.D. Stout, C. Burda, Y. Lou, X. Chen, *J. Phys. Chem. B* 108 (2004) 1230–1240.
- [14] J. Yu, M. Zhou, B. Cheng, X. Zhao, *J. Mol. Catal. A* 246 (2006) 176–184.
- [15] S. Yin, K. Ihara, Y. Aita, M. Komatsu, T. Sato, *J. Photochem. Photobiol. A* 179 (2006) 105–114.
- [16] J.A. Rengifo-Herrera, E. Mielczarski, J. Mielczarski, N.C. Castillo, J. Kiwi, C. Pulgarin, *Appl. Catal. B* 84 (2008) 448–456.
- [17] R. Asahi, T. Morikawa, T. Ohwaki, K. Aoki, Y. Taga, *Science* 293 (2001) 269–271.
- [18] E. Finazzi, C. Di Valentini, A. Selloni, G. Pacchioni, *J. Phys. Chem. C* 111 (2007) 9275–9282.
- [19] Q. Li, J. Xue, W. Liang, J.-H. Huang, J.K. Shang, *Phil. Mag. Lett.* 88 (2008) 231–238.
- [20] M. Sathish, B. Viswanathan, R.P. Viswanath, C.S. Gopinath, *Chem. Mater.* 17 (2005) 6349–6353.
- [21] H. Sun, Y. Bain, Y. Cheng, W. Jin, N. Xu, *Ind. Eng. Chem. Res.* 45 (2006) 4971–4976.
- [22] G. Colon, M.C. Hidalgo, G. Munera, I. Ferino, M.G. Cutrufello, J.A. Navio, *Appl. Catal. A* 63 (2006) 45–59.
- [23] S. Sakhivel, M. Janczarek, H. Kisch, *J. Phys. Chem. B* 108 (2004) 19384–19387.
- [24] W. Ho, J.C. Yu, S. Lee, *J. Solid State Chem.* 179 (2006) 1171–1176.
- [25] H. Fu, L. Zhang, Y. Zhu, J. Zhao, *J. Phys. Chem. B* 110 (2006) 3061–3065.
- [26] S. Liu, X. Chen, J. Hazard. Mater. 152 (2008) 48–55.
- [27] M. Mrowetz, W. Balcerki, A.J. Colussi, M.R. Hoffmann, *J. Phys. Chem. B* 108 (2004) 17269–17273.
- [28] S. Livraghi, M.C. Paganini, E. Giambello, A. Selloni, C. Di Valentini, G. Pacchioni, *J. Am. Chem. Soc.* 128 (2006) 15666–15671.
- [29] T. Tachikawa, S. Tojo, K. Kawai, M. Endo, M. Fujitsuka, T. Ohno, K. Nishijima, Z. Miyamoto, T. Majima, *J. Phys. Chem. B* 108 (2004) 19299–19306.
- [30] Y. Liu, J. Li, X. Qiu, C. Burda, *J. Photochem. Photobiol. A* 190 (2007) 94–100.
- [31] D. Mitraj, A. Jańczyk, M. Strus, H. Kisch, G. Stochel, P.B. Heczko, W. Macyk, *Photochem. Photobiol. Sci.* 6 (2007) 642–648.
- [32] Q. Li, R. Xie, Y.W. Li, E.A. Mintz, J.K. Shang, *Environ. Sci. Technol.* 41 (2007) 5050–5056.
- [33] Y. Lion, M. Delmelle, A. Van der Vorst, *Nature* 263 (1976) 442–443.
- [34] T. Ando, T. Yoshikawa, T. Tanigawa, M. Kohno, N. Yoshida, M. Kondo, *Life Sci.* 61 (1997) 1953–1959.
- [35] A. Nambu, J. Graciani, J.A. Rodriguez, Q. Wu, E. Fujita, J.J. Fernandez-Sanz, *Chem. Phys.* 125 (2006) 094706–1–094706–8.
- [36] O. Diwald, T.L. Thompson, E.G. Goralski, S.D. Walck, J.T. Yates, *J. Phys. Chem. B* 108 (2004) 52–57.
- [37] N.C. Saha, H.G. Tompkins, *J. Appl. Phys.* 72 (1992) 3072–3079.
- [38] O. Diwald, T.L. Thompson, E.G. Goralski, S.D. Walck, J.T. Yates, *J. Phys. Chem. B* 108 (2004) 6004–6008.
- [39] H. Sun, Y. Bai, Y. Cheng, W. Jin, N. Xu, *Ind. Eng. Chem. Res.* 45 (2006) 4971–4976.
- [40] L.K. Randeniya, A.B. Murphy, I.C. Plumb, *J. Mater. Sci.* 43 (2008) 1389–1399.
- [41] T. Umebayashi, T. Yamaki, H. Itoh, K. Asai, *Appl. Phys. Lett.* 81 (2002) 454–456.
- [42] T. Umebayashi, T. Yamaki, A. Yamamoto, A. Miyashita, S. Tanaka, T. Sumita, K. Asai, *J. Appl. Phys.* 93 (2003) 5156–5160.
- [43] E.L.D. Hebenstreit, W. Hebenstreit, U. Diebold, *Surf. Sci.* 470 (2001) 347–360.
- [44] D. Chatterjee, S. Dasgupta, *J. Photochem. Photobiol. C* 6 (2006) 186–205.
- [45] I. Ilisz, A. Dombi, *Appl. Catal. A* 180 (1999) 35–45.
- [46] A. Sobczyński, L. Duczmal, W. Zmudzinski, *J. Mol. Catal. A* 213 (2004) 225–230.
- [47] R.W. Matthews, S.R. McEvoy, *J. Photochem. Photobiol. A* 64 (1992) 231–246.
- [48] R. Enriquez, A.G. Agrios, P. Pichat, *Catal. Today* 120 (2007) 196–202.
- [49] C.S. Zalazar, C.A. Martin, A.E. Cassano, *Chem. Eng. Sci.* 60 (2005) 4311–4322.
- [50] R. Enriquez, P. Pichat, *J. Environ. Sci. Health A* 41 (2006) 955–966.
- [51] H. Noda, K. Oikawa, H. Kamada, *Bull. Chem. Soc. Jpn.* 66 (1993) 455–458.
- [52] S. Kim, W. Choi, *J. Phys. Chem. B* 109 (2005) 5143–5149.
- [53] A.G. Rincon, C. Pulgarin, *Appl. Catal. B* 44 (2003) 263–284.
- [54] G.R. Hodges, K.U. Ingold, *Free Radic. Res.* 33 (2000) 547–550.
- [55] W. Macyk, H. Kisch, *Chem. Eur. J.* 7 (2001) 1862–1867.
- [56] R. Konaka, E. Kasahara, W.C. Dunlap, Y. Yamamoto, K. Cheng-Chien, M. Inoue, *Redox Rep.* 6 (2001) 319–325.
- [57] B. Vileno, M. Lekka, A. Sienkiewicz, P. Marcoux, A.J. Kulik, S. Kasas, S. Catsicas, A. Gaczyk, L. Forró, *J. Phys. Condens. Matter* 17 (2005) S1471–S1482.
- [58] L.K. Andersen, P.R. Ogilby, *J. Phys. Chem. A* 106 (2002) 11064–11069.
- [59] Y. Nosaka, T. Daimon, A.Y. Nosaka, Y. Murakami, *Phys. Chem. Chem. Phys.* 6 (2004) 2917–2918.
- [60] K. Hirakawa, T. Hirano, *Chem. Lett.* 35 (2006) 832–833.
- [61] T. Daimon, Y. Nosaka, *J. Phys. Chem. C* 111 (2007) 4420–4424.
- [62] T. Daimon, T. Hirakawa, M. Kitazawa, J. Suetake, Y. Nosaka, *Appl. Catal. A* 340 (2008) 169–175.
- [63] K. Naito, T. Tachikawa, M. Fujitsuka, T. Majima, *J. Phys. Chem. C* 112 (2008) 1048–1059.
- [64] D.T. Sawyer, *Acc. Chem. Res.* 14 (1981) 393–400.
- [65] A. Fujishima, T.N. Rao, D.A. Tryk, *J. Photochem. Photobiol. C* 1 (2000) 1–21.
- [66] Z. Cheng, Y. Li, *Chem. Rev.* 107 (2007) 748–766.
- [67] T.A. Dahl, W.R. Midden, P.E. Hartman, *Photochem. Photobiol.* 46 (1987) 345–352.
- [68] C. Li, M.Z. Hoffman, *J. Phys. Chem. A* 104 (2000) 5998–6002.